Nanotechnology

PURPOSE-LED PUBLISHING™

PAPER

Single-nanowire-morphed mechanical slingshot for directional shooting delivery of micro-payloads

To cite this article: Ying Zhang *et al* 2023 *Nanotechnology* **34** 415604

View the article online for updates and enhancements.

You may also like

- Engineering in-plane silicon nanowire springs for highly stretchable electronics
Zhaoguo Xue, Taige Dong, Zhimin Zhu et al.
- Ultra-high aspect ratio Si nanowires fabricated with plasma etching: plasma processing, mechanical stability analysis against adhesion and capillary forces and oleophobicity
A Zeniou, K Ellinas, A Olziersky et al.
- An analytical-atomistic model for elastic behavior of silicon nanowires
Sina Zare Pakzad, Mohammad Nasr Esfahani and B Erdem Alaca

This content was downloaded from IP address 202.119.48.217 on 05/11/2026 at 03:13

IOP Publishing Nanotechnology
Nanotechnology 34 (2023) 415604 (9pp) https://doi.org/10.1088/1361-6528/ace5b5

Single-nanowire-morphed mechanical slingshot for directional shooting delivery of micro-payloads

Ying Zhang, Jiang Yan, Dianlun Li, Wentao Qian, Yongjia Qi, Lei Wu, Zongguang Liu, Junzhuan Wang, Jun Xu and Linwei Yu

National Laboratory of Solid State Microstructures, School of Electronics Science and Engineering, Nanjing University, Nanjing, 210093, People's Republic of China

E-mail: yulinwei@nju.edu.cn

Received 17 May 2023, revised 3 July 2023
Accepted for publication 10 July 2023
Published 27 July 2023

Abstract

Stretching elastomer bands to accumulate strain energy, for a sudden projectile launching, has been an old hunting skill that will continue to find new applications in miniaturized worlds. In this work, we explore the use of highly resilient and geometry-tailored ultrathin crystalline silicon nanowires (SiNWs) as elastic medium to fabricate the first, and the smallest, mechanical slingshot. These NW-morphed slingshots were first grown on a planar surface, with desired layout, and then mounted upon standing pillar frames, with a unique self-hooking structure that allows for a facile and reliable assembly, loading and shooting maneuver of microsphere payloads. Impressively, the elastic spring design can help to store 10 times more strain energy into the NW springs, compared with the straight ones under the same pulling force, which has been strong enough to overcome the sticky van der Waals (vdW) force at the touching interfaces that otherwise will hinder a reliable releasing onto soft surface with low-surface energy or adhesion force, and to achieve a directional shooting delivery of precise amount of tiny payload units onto delicate target with the least impact damage. This NW-morphing construction strategy also provides a generic protocol/platform to fast design, prototype, and deploy new nanoelectromechanical and biological applications at extremely low costs.

Supplementary material for this article is available online

Keywords: IPSLS growth, silicon nanowires, 3D assembly, mechanical shooting-release

(Some figures may appear in colour only in the online journal)

1. Introduction

The last decade has witnessed a rapid increase of research efforts devoted to the microscale manipulation [1, 2], transport [3, 4] and injection [5, 6] of tiny objects for advanced superstructure assembly, nanoelectromechanical detection, drug delivery or genetic therapy [7–15], where a precise amount of discrete inorganic or biological payloads need to be delivered or attached to target objects of a cell [16], organ [17, 18] or Nanoelectromechanical systems(NEMS) sensing units [19]. With the size shrinkage of size into microscale, the manipulation of tiny objects is increasingly subject to the influence of interfacial adhesive forces, arising from capillary, electrostatic or van der Waals forces, which could hinder an effective release or delivery of tiny *functional bullets* onto targeted objects or locations. In order to address this challenge, many approaches have been proposed and can be classified into passive or active releasing modes [20]. For the passive mode, it relies on a large adhesive force at the payload/target interface, greater than that of the payload/holder interface, to enforce a transfer of the carried object onto the target surface. This approach has been proved to be effective but applicable only to a specific combination of target/object materials [7, 21]; for the active modes, the payload objects can be manipulated by non-contacted external magnetic field or optical tweezers [22–25], or directly held by

© 2023 IOP Publishing Ltd
All rights, including for text and data mining, AI training, and similar technologies, are reserved.

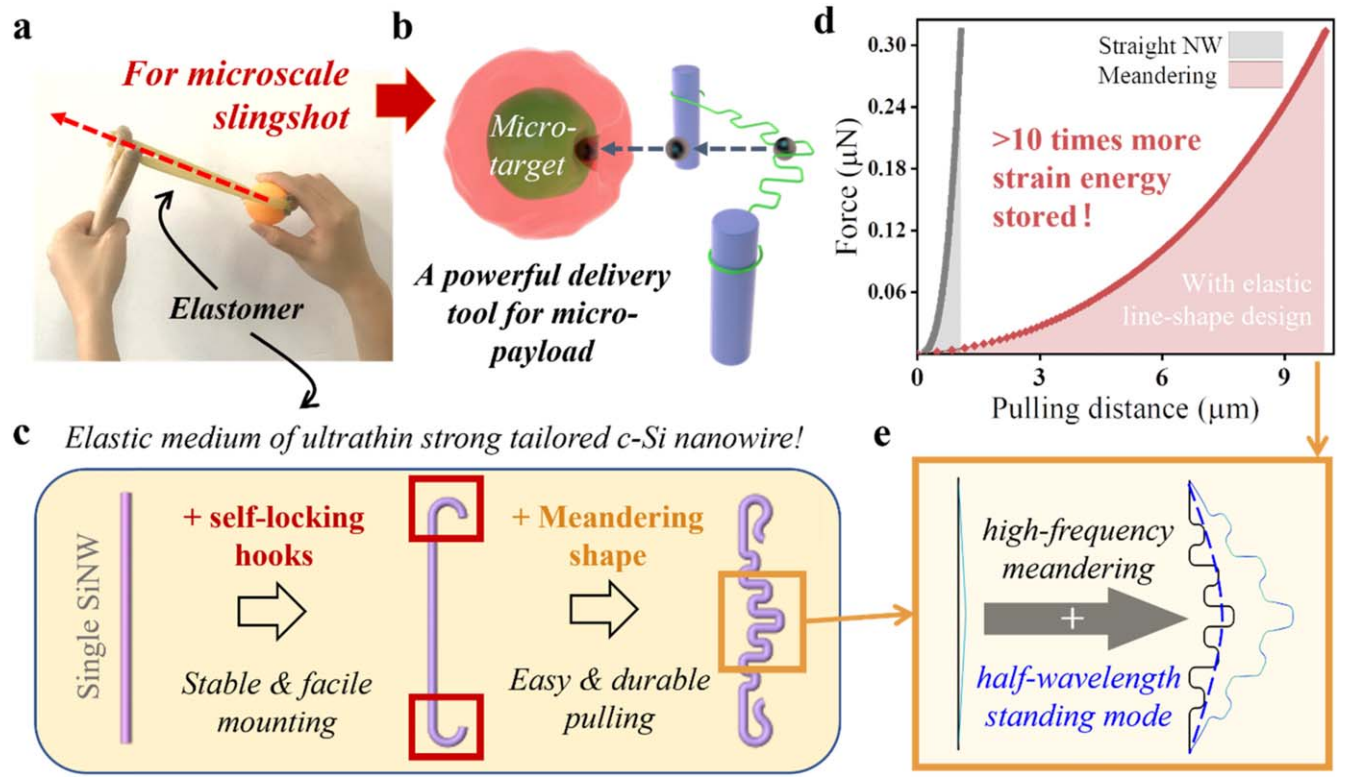


Figure 1. Schematic diagram of Single NW-morphed mechanical slingshot. (a), (b) A comparison of the structural similarity and designs of macroscale and microscale slingshots. (c) The elastic medium is replaced by rigid/strong but slim c-Si NW in microscale slingshot, with self-locking hook ends and a meandering spring shape to boost largely the strain energy stored in a deformed/pulled NW slingshot. (d), (e) Finite element mechanical simulation reveals that the stored strain energy in meandering NW spring can be 10 times more than that in straight one, based an optimized line-shape design that superimposes a small amplitude high-frequency meandering upon a long (half)-wavelength standing-mode spring.

micro-grippers that can be excited into resonant vibration to release the holding object [20, 26]. Despite of these successful demonstrations, by using expensive nano-manipulator setups and in specific instrumental environments, it is still desirable to explore a more facile, economic and straightforward technique to achieve an efficient micro payload delivery.

To this end, one of the oldest hunting skills in human history, *mechanical shooting*, could continue to step in and help in the miniaturized world. Recently, the launching of micro particles has been realized in hollow micro cannon structures powered by ultrasonic triggered bursting reaction [27], while intriguing DNA-based slingshots were fabricated by combining antibody handles and synthetic DNA strands in molecular level, serving as a stretchy band to deliver cancer-combating drug payloads onto the surface of tumor cells [28]. All these works point to the advantage of achieving a straightforward shooting delivery of micro/nano-scale payloads, while a genuine mechanical slingshot, with elastic bands hinged to pillar frames, has never been fabricated in microscale. This is nontrivial as it could offer a powerful means to integrate a small but easy-to-control pulling force, over a long enough distance, to accumulate sufficient strain energy for a shooting-release of micro-payload, overcoming the adhesive interfacial forces and shooting into desired aiming direction.

Unfortunately, it is impractical to downscale the rubber-band-powered slingshot (see figure 1(a) for example) directly into microscale, as the ultrathin elastic string medium has to be highly durable, resilient and suitable for aggressive size-scaling into sub-microscale. A good candidate is the quasi-one-dimensional (1D) crystalline silicon nanowires (SiNWs), which can store a high density of strain energy to a level comparable to the volumetric energy density of TNT (trinitrotoluene) [29]. Though suspended slim c-Si beams and cantilevers, with width ~100 nm, have been widely used in many NEMS applications [30], they need to be etched out of expensive SOI wafer with the aid of high precision but expensive electron beam lithography (EBL), not to mention the challenges in reliable suspension, transfer and pillar-frame mounting. On the other hand, c-Si by itself is brittle and prone to break under tiny tensile strain, up to 0.3%, even in form of straight SiNW, up to 1% [31, 32]. In order to sustain the large stretching, ideally >30% required for controllable loading, pulling and shooting of slingshot, the slim SiNW spring needs to be engineered into suitable elastic form, which poses as another challenge for conventional large-scale and high precision fabrication.

In this work, we explore a single-SiNW-morphing strategy to batch-fabricate designable microscale slingshots, with designable ultralong SiNWs as elastic springs, which were grown via an in-plane solid–liquid–solid (IPSLS) mechanism established in our previous works [33–35]. A facile and reliable 3D mounting of the SiNW springs upon standing pillars were accomplished thanks to a unified self-

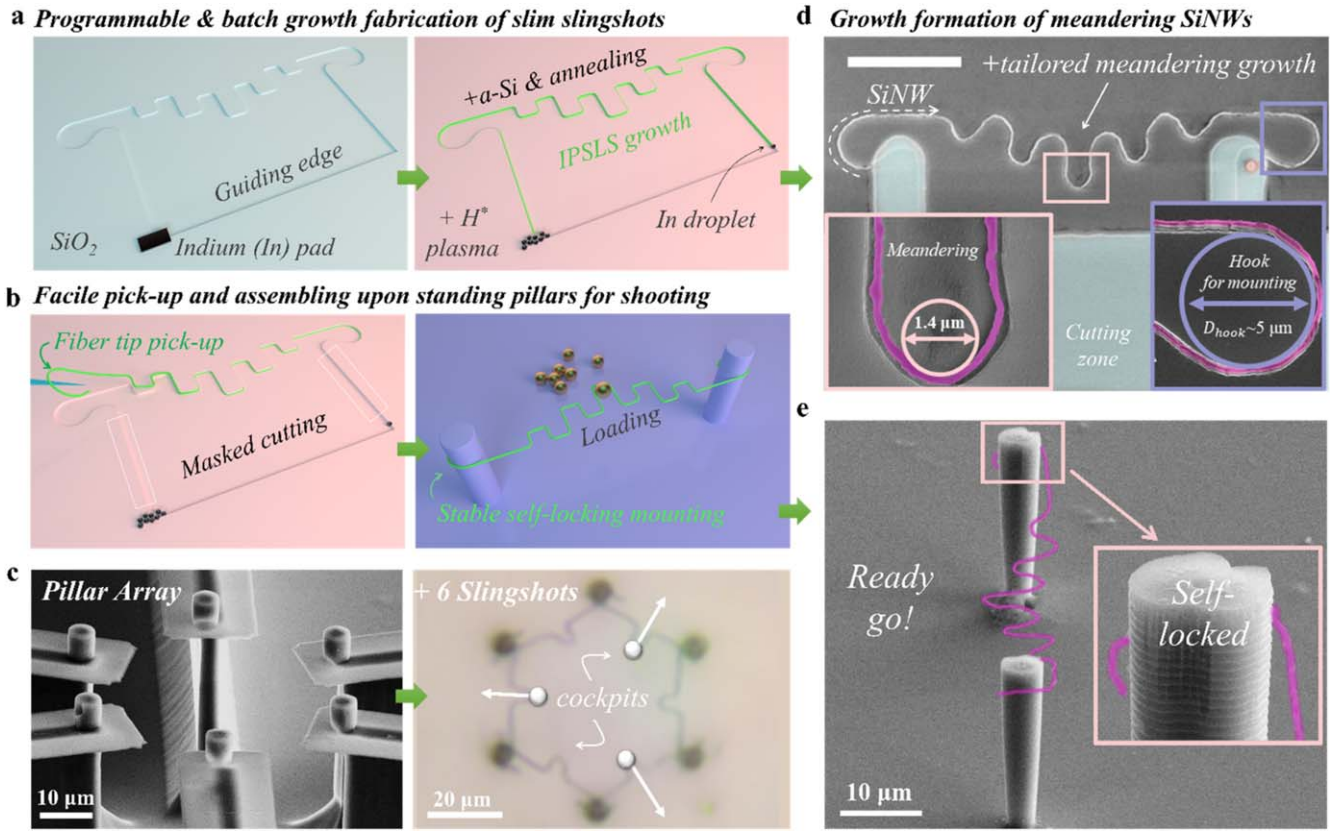


Figure 2. IPSLS growth and assembly of NW slingshots. (a) illustrates schematically the guided growth of c-Si NWs via IPSLS mode, led by indium (In) droplets that consume a-Si layer as precursor, following the pre-defined step edges during a low temperature annealing in vacuum. (b) Fiber tip assisted picking and transferring of as-grown c-Si NWs, and mounting them upon a pair of pillar frames, with a cockpit site for the loading of microsphere in the center. (c) showcases the assembly of 6 slingshots upon a group of more complex hexagonal arrays of standing pillars, thanks to the facile and reliable self-locking and mounting mechanism. (d) SEM images of the NW spring with ideal meandering shape, where the left inset shows a close view of the center cockpit while the right one examines one of the as-grown NW hooky ends, prior to final cutting. The scale bar in (d) stands for 10 μm. (e) shows a sideview SEM image of a single NW slingshot installed upon Bosch-etched pillars, with clear sidewall grooves as seen in the inset.

locking spring-hook structure, as depicted in figure 1(b), while an elastic line-shape design can help to achieve more than 10 times larger strain energy in the SiNW springs, compared to the straight ones. These unique combined capabilities enable the first successful demonstration of a real mechanical slingshot in microscale, which can be successfully loaded with microscale payload model of SiO_2 spheres, of ~3–5 μm in ambient conditions, and triggered to shoot and release, with an adjustable angle and distance control, providing an extremely facile but powerful and diverse platform for rapid design, prototyping and testifying various microscale mechanical manipulation/injection concepts and functionalities.

2. Results and discussion

2.1. Design principle and fabrication of SiNW-morphed slingshots

In order to *replicate* a functional slingshot in microscale, as envisioned in figures 1(a)–(b), a pair of standing pillars of 4 μm wide, 2 μm height and 50 μm apart, was first etched out of Si wafer (heavily doped) via a standard Bosch procedure, to serve as the microscale frames *holding* the SiNW spring. Note that the Bosch etching is a well-known deep-etching technology that leaves periodic scallop-shaped grooves on the pillar sidewalls, with alternating etchant periods of SF_6 and C_4F_8 gases [36], as witnessed in figure S1 and explained with more details in the experimental section. The SiNW springs were grown via an IPSLS mechanism [33], led by indium (In) catalyst droplets that consume surface-coating amorphous Si (a-Si) thin film as a precursor to produce crystalline SiNWs along their moving courses. During the IPSLS growth, the In catalyst droplets can be attracted and directed by pre-defined step edges [34, 35], as illustrated in figure 2(a), to produce SiNWs at the desired locations with designable line-shapes. More growth mechanism and experimental details are available in our previous works and in the Method sections.

Actually, there are two major challenges that need to be addressed in the design, fabrication and assembly of a microscale slingshot. The first one is how to engineer an elastic shape for the suspended SiNW spring to store more strain energy given a constant pulling strength, while allowing for maneuverable or easy-to-handle loading, pulling and shooting operations. Apparently, a straight SiNW spring, as

seen in the far-left panel of figure 1(c), is the simplest and easy-to-conceive spring form, but it allows for only a very limited lateral displacement pulling distance, and thus easy to break even with the greatest care (of manual operation), due to the rigid and brittle nature of c-Si even in 1D form. So, a *meandering* or wavy spring shape has been adopted here that helps to convert the overall stretching strain into local bending, which can be better accommodated by the slim SiNWs. An extra bonus is that a stable cockpit site can be formed at the center of SiNW spring, which is beneficial for a reliable loading of microspheres, as well as a convenient handle-end for fiber-tip manipulation.

More importantly, according to the finite element mechanical analysis in figures 1(d)–(e), the maximal strain energy stored in the elastic meandering SiNW spring can be greatly improved, by more than 10 times larger, with respect to that in a straight one, under the same pulling force. This can be inferred from the force-displacement plot in figure 1(d), where the underlying areas of the increasing force-displacement curves represent the stored mechanical energies for the meandering or straight SiNW springs. Note that, the elastic line-shape engineering of the SiNWs makes it possible to substantially reduce the resilience strength of the SiNW springs, that is, making it much *softer* with greatly reduced equivalent Hooke coefficient (k), which can be seen clearly from the simulated force response in figure 1(d), where the spring-shaped nanowire can be stretched or pulled to much longer distance under the same pulling force. According to the Hooke's law, the accumulative strain energy stored into a pulled nanowire spring can be roughly estimated by $W = F^2/2k$, where F is the applied pulling force. So, a *softer* spring of tailored SiNWs, with a lower k, will store much more mechanical energy, compared with the straight ones. Also, the effective Hooke coefficient of the SiNW spring, that's the slope of the force-pulling displacement curve, is not always a constant, but gradually increases under large pulling. This is also the fundamental reason why a wavy SiNW spring can help to store much more strain energy for achieving an effective shooting, as indeed observed in this work. Of course, the stored energy can be further increased by increasing the meandering amplitude, but in that case, the suspended SiNWs will become too soft to be self-sustainable against gravity dragging. Taking these factors into account, an optimized spring shape has been obtained, which features a *high-frequency* but small amplitude meandering design superimposed upon a *half-wavelength* standing mode spanning the two supporting pillars, as diagramed in figure 1(e). More structural analysis and evolution of the SiNW slingshots are provided in figure S2.

Fortunately, these meandering SiNW springs can be obtained via a single run of IPSLS growth, as seen for example in the SEM image shown in figure 2(d), where an ultralong SiNW pseudo-colored to purple, with a diameter and length of 130 ± 20 nm and >100 μm respectively, were directed or introduced from a remote In pad (out of the SEM view) into the slingshot-shaping guiding zone. Thanks to a stable guided growth, the SiNWs grew steadily over the curved edges with the smallest turning radius down to r_{nw} < 0.7 μm at the center cockpit, as seen in the left inset. Note that, according to the Raman spectroscopy characterization of the as-grown SiNW spring, as shown in figure S3, it is of polycrystalline c-Si with a Raman peak at ~519.4 cm^{-1} nm and a full width at half maximum (FWHM) <6 cm^{-1}. This is consistent with the high-resolution transmission electron microscopy examination of the similar geometry-tailored IPSLS SiNWs, as witnessed in our previous work [35].

The second challenge is how to pick up and transfer or mount the slim SiNW spring stably onto the standing pillar frame, for rapid prototyping of slingshot functionality. Here, a sharp fiber tip, with a diameter of 200 nm at the tip and manually controlled via a microprobe stage, was used as the tool to approach and pick up the SiNWs from their parent substrate, mainly with the aid of adhesive vdW force at the touching interface. In order to guarantee a stable and flexible enough hinging connection of the SiNW spring to the pillar frame, a self-locking hook design has been composed and realized at the ends of the springs, see the schematic diagram and SEM image in figures 1(c) and 2(d), which exempts the needs of extra sticky paste or soldering medium that could complicate or contaminate the simple 3D slingshot structure. Note that the formation of such *hooking* ends was accomplished by cutting off the outer side of an open circle guiding track, as indicated in the inset of figure 2(d), which is designed to have a diameter ~20% larger than that of the standing pillars. In this way, the hook ends can be easily manipulated to fit and clasp around the pillar tops, while the pillar separation is set to ~4% wider than the full span of the slingshot to introduce a beneficial stretching force that further stabilize the mounting of the SiNW spring in suspension. More interestingly, the Bosch-etched rough sidewall grooves (see the inset of figure 2(e)) can also serve as helpful notch lines to fix the suspended SiNW at variable height. To demonstrate the efficiency and reliability of such a picking-and-mounting technology, a video clip of the whole assembly process has been provided in supplementary video S1, while this facile 3D assembly can even be applicable to fabricate more complex orderly array of 6 SiNW springs suspended among hexagonal pillar frame (figure 2(c)).

2.2. SiNW-morphed slingshots shooting demonstration

The SiNW slingshot shooting was carried out by using a manually controlled fiber tip, preloaded with a microsphere of 4 μm wide, and observed under an optical microscope, as schematically diagrammed in figure 3(a). As seen in the captured image clips in figure 3(b), during the loading process, a slightly inclined fiber tip, ~15° to the ground, was moved to approach to the SiNW spring, touch the center cockpit and draw it over a pulling distance of $\boldsymbol{l_d \sim 8\ \mu m}$. As the fiber is much thinner than the meandering wavelength, the much wider microsphere payload can be effectively passed onto/or stuck to the protruding segments of the SiNW spring, in the gradual stretching stage. After pulling to a long enough distance, a sudden shooting of the microsphere bullet can be triggered due to a slipping release of the deformed spring from the inclined fiber tip. Thanks to a reliable self-locked hooking and the resilient nature of c-Si NW spring, this

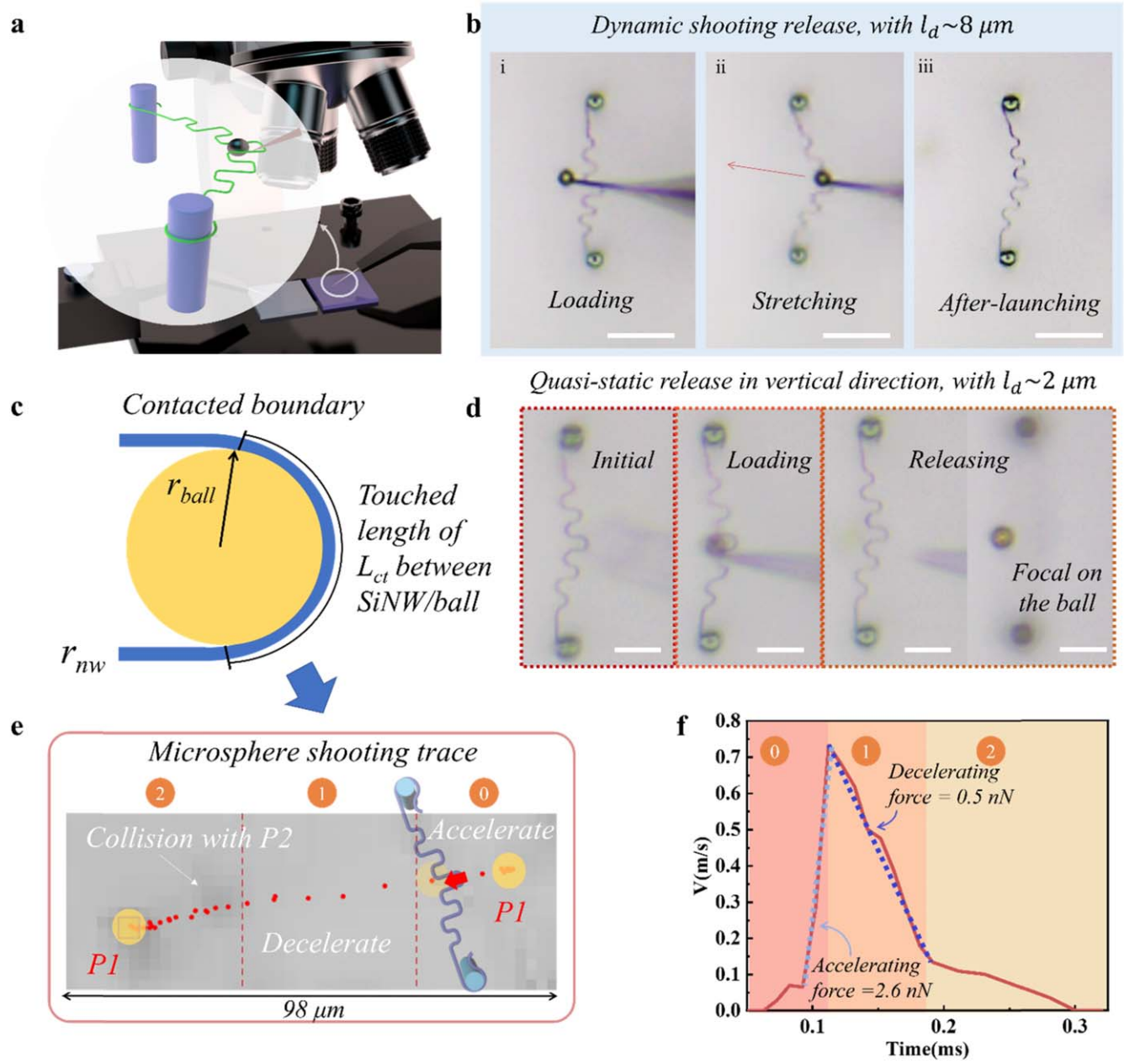


Figure 3. Elastic shooting release testing. (a) sketches the home-made and manually controlled manipulation and observation platform used to testify the NW slingshot shooting and releasing operations, where (b) shows the photoshoots of a fiber tip picking up a microsphere payload, loading it to a poised NW slingshot, stretching to approximately 8 μm apart and shooting to the left direction. Scale bars are for 20 μm. Another quasi-static shooting release of a loaded microsphere onto the ground surface is shown in (d), where the pulling distance is reduced to 2 μm, the scale bars are for 10 μm. (c) depicts the estimation of the maximal contacted length *L*_ct between the touched NW spring and the loaded microsphere. (e)–(f) show the moving trajectory and the extracted velocity evolution of a slingshot shooting of microsphere with three distinctive Stages.

microscale slingshot is readily reusable, with only slight deformation after the first shooting operation. Note that, by adjusting the incline angle and the initial contact position, the slingshot can also be controlled to release the microsphere quasi-statically just in front of the spring. Such an example is demonstrated in figure 3(d), where a shorter pulling distance over $\boldsymbol{l_d \sim 2\ \mu m}$, generated by adopting a larger incline angle and lighter pressing contact between the fiber tip and the spring, leads to a basically vertical releasing of the microsphere, as inferred from the focused-and-defocused images.

In order to gain more dynamic details of the slingshot shooting, a high-speed camera (Phanton VEO 1310L, 10^5 frames per second) has been used to track the motion trajectory of the launched projectile. As shown in a wide-angle image of figure 3(e), (a) microsphere was shot by a slingshot from right to left, traveling over a distance of over ~80 $\boldsymbol{\mu m}$, as shown in video S2†, from which the velocity evolution of the micro-projectile can be extracted and plotted at different time in figure 3(f). There are apparently three stages that can be discerned from this velocity-time plot, which include

accelerating Stage 0, from $t = 0$ to 0.11 ms, where the microsphere was observed to experience a quasi-linear acceleration, up to $v_{max} = 0.73\,\mathrm{m\,s^{-1}}$, with a deduced corresponding driving force exerted by the elastic spring of $F_{acc} \sim 2.6\,\mathbf{nN}$, assuming the payload mass of $m = 8 \times 10^{-5}\,\mu\mathrm{g}$. After that, most likely due to frictional environmental forces imposed by the ground, electrostatic or air impedances, it turned into a linear and fast decelerating Stage 1, where the dragging force can be estimated to be around $F_{dec} \sim 0.5\,\mathbf{nN}$, which manifested after the detaching of microsphere from the spring. At the end, after colliding with another static microsphere sitting in its way, it came to halt in a gentle slow-down Stage 2, as marked in figure 3(e).

Considering the pulling distance of $l_d \sim 10\,\mu\mathrm{m}$, the installed strain energy can be estimated to be around $E_{el} = 980\,\mathbf{fJ}$. Prior to the detaching, at the transit from Stage 0 to 1, the kinetic energy gained by the microsphere is only

$$E_{ki} = \frac{1}{2} m v_{\max}^2 \sim 21\,\mathbf{fJ}, \tag{1}$$

which accounts for only a small fraction of the elastic energy of the SiNW spring. This also indicates that most of the elastic energy has been lost against the frictional forces during the shooting process. But, it is also intriguing to speculate that, if all these frictional losses can be warded off, and the slingshot is pulled to the failure limit of c-Si NW (to a maximum stress of 18 GPa) [29], the stored strain energy should be sufficient to accelerate a 4 μm-sized PS sphere payload to a maximum speed of $>22\,\mathrm{m\,s^{-1}}$.

On the other hand, for the contact length (L_{ct}) between the microsphere and spring, the vdW force between them can be roughly estimated [37, 38], according to the configuration as sketched in figure 2(c), to be

$$F_{vdw} = \frac{L_{ct}}{\Delta L} \frac{2A r_{ball}^3}{3(2r_{ball} + s_0)^2 s_0^2} \left(\frac{r_{nw}}{r_{nw} + r_{ball} + s_0} \right)^{\frac{1}{2}} \sim 2.35\,\mu\mathbf{N}, \tag{2}$$

where L_{ct} is the full contact length between the NW spring and the microsphere, $\Delta L \sim 0.25\, r_{ball}$, A the Hamaker constant estimated to be $\sim$13 zJ [39], r_{ball} the radius of the sphere of approximately 2 μm, r_{nw} the radius of the NW of $\sim$60 nm, and s_0 the equilibrium separation distance between the NW and sphere, estimated to be 0.2 nm [40]. So, the corresponding work (E_v) needed to overcome the vdW force at the contact boundary should be around

$$E_v = \frac{s}{2} F_{vdw} = 12\,\mathbf{fJ}, \tag{3}$$

where S is the vdW force cut-off distance between the NW and the microsphere of $\sim$10 nm. Apparently, the vdW force barrier falls far below the total strain energy stored in the NW spring, and also less than the gained kinetic energy of the accelerated microsphere. In other words, the shooting-releasing can be powerful enough to overcome the sticky vdW attraction to deliver a microscale payload towards desired location and direction.

2.3. Directional shooting operation

Though this highly miniaturized NW-slingshot prototype is far from being a precise projecting tool, due to the manually controlled loading, pulling and firing processes, it does demonstrate a primitive but still impressive capability of directional shooting onto aimed targets. As showcased in figure 4(a), a free-fire shooting of microsphere bullets into front open area have been repetitively carried out for 10 times, by using the same slingshot. The fiber tip imposed pulling distances has been controlled to be roughly the same $l_d \sim 12\,\mu\mathbf{m}$, with constant incline angle of $\sim$15°, but free shooting directions. According to the statistics shown in figure 4(b), the shooting distance L_{shoot} is $100 \pm 28\,\mu\mathbf{m}$ with a spreading angle ranging from −41° to +31°, with respect to the center normal. Note that, the shooting angle of the fixed slingshot setup is adjustable, as the elastic SiNW spring can also be stretched into tilted direction, with deviation angle of $\theta_{\mathbf{d}}$ as depicted in the inset of figure 4(c), but still work as a directional shooter. This wide-angle-shooting capability, probably desired in practical delivery or feeding scenarios, is derived from the superimposed meandering design in the SiNW spring, where a tilted pulling will lead to asymmetric but still elastic deformations in the upper and lower spring segments, as witnessed in the finite element simulation shown in the figure 4(c), except that the force responses may vary to some extent depending on the stretching direction and distance.

This microscale mechanical slingshot was also testified to aim and attack microscale targets. As shown in figures 4(d)–(e), a strong but somehow deviated sidewall impinging of a micro bullet (marked by blue) onto a static target of similar size (red) demonstrate a quasi-ballistic collision, while a normal incidence, with somehow less strength, can be result in an adhesive sticking of the microscale target and bullet. More operational details are available in video S3 and video S4. These two situations could both find useful applications in practical applications, for example, to eliminate undesired target (by strong ballistic shooting) or to install tiny mechanical payload for sensing [41] or deliver medicine or genetic cues [15, 42]. To further exemplify this functionality, a simple bio-target shooting was carried out, where a side-flipped algal cell (15 μm wide and 20 μm long) was selected as the target, sitting 55 μm away from the slingshot. Figure 4(f) shows only the final state that a model microsphere payload has been directly and reliably delivered to stick to the cell sidewall via a single loading and shooting operation, more details are available in video S5†. Note that this rapid and clear-cut shooting-delivery involves basically no vdW force exchange, or direct dragging and force-competition between the transport tool, payload and the target. This can be very helpful particularly for attaching precise amount of tiny bio or inorganic payload object, directly onto irregular, soft and even low-surface-energy target surfaces with the minimal damage impact.

In view of future scalable fabrication and integration, the ultra slim SiNW springs ($\sim$100 nm in diameter) can be batch-manufactured, as orderly array upon various substrate

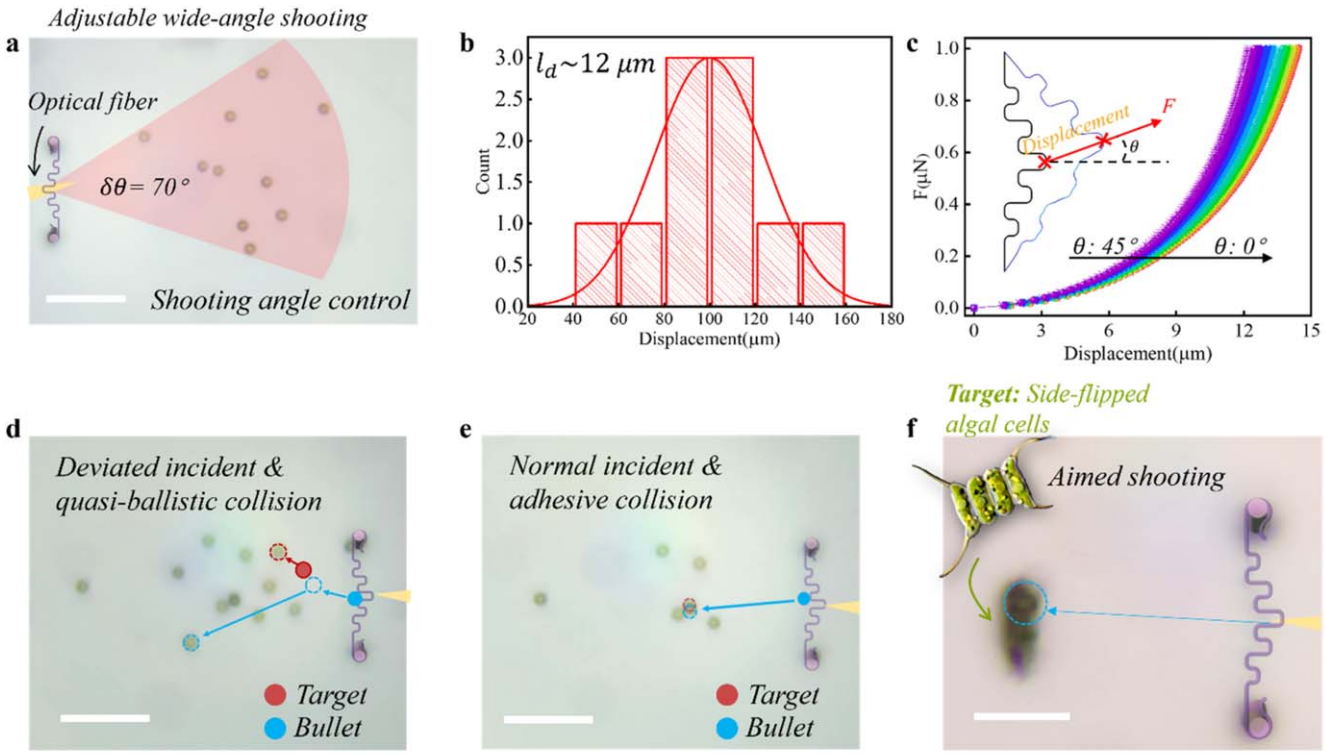


Figure 4. Aimed shooting by NW slingshot. (a) Photo of the spread of the shot microspheres in the front field after 10 repetitive shootings by using the same slingshot setup on the left, while a statistic on the shooting distance distribution is provided in (b) Scale bar in (a) stands for 50 μm. c. simulated force-displacement response analysis for shooting into varied tilted angle ranging from 0 to 45 degrees. (d), (e) show the captured images of a quasi-ballistic and adhesive collisions between the target and bullet microspheres. (f) showcases a successful shooting transport of a model microsphere bullet to stick on the surface of a side-flipped algal cells. Scale bars in (d), (e) and (f) stand for 50 μm and 20 μm, respectively.

surfaces, including wafer, glass or even polymer, thanks to the low temperature IPSLS growth of Si nanowires at <350 ℃, and without the need of sophisticated EBL or DUV lithography; then, the SiNW springs could be fixed at the two ends and suspended via selective etching of the targeted underlying substrate layers, via the established NEMS technologies that have been widely used in the literature [43], while a more precise loading and shooting of projectiles could be accomplished via commercially available automatic robotic system [44] or the finger-like SiNW-morphed nano grippers recently demonstrated in our group [45].

3. Conclusions

In summary, we have successfully demonstrated a designable fabrication and assembly of the smallest full-function mechanical slingshot, by adopting ultralong and ultrathin Si NWs as elastic medium, which were obtained via a guided IPSLS growth. The NW-morphed slingshots feature a unique self-locking hook end structure that greatly facilitates a reliable 3D mounting upon standing pillar pairs, while the tailored elastic meandering spring shape allows accumulating 10 times more strain energy, compared to the straight spring under the same pulling force, which can be strong enough to overcome the sticky vdW force barrier for reliable and straightforward shooting delivery of micro-payload to various low-surface energy surfaces, with a reasonably tunable shooting direction and distance control. This miniaturized mechanical slingshot could find potential applications in NEMS sensing, biological delivery or medicine therapy treatment, while indicating also a whole new facile and generic protocol to rapidly construct and prototype other 3D mechanical designs and functionalities.

4. Experimental

4.1. Growth of SiNWs by IPSLS

The SiNW springs of the slingshots were grown on SiO_2 (500 nm) -coated c-Si wafers, via an IPSLS mechanism [33–35], which involves (1) the patterning of guiding edges by using conventional photolithography to define the shape of a slingshot and subsequent inductively coupled plasma (ICP) etching to form a growing sidewall, with SF_6 etchant gas, for around 120 nm into the SiO_2 layer. Note that, the line-shape of the slingshot is defined by the layout of the guiding edge lines. (2) The deposition of 35 nm thick In catalyst strip across the starting ends of the guiding edges, via lithography and electron beam evaporation of In, followed by standard lift-off process; (3) the deposition of 30 nm a-Si layer on the whole sample surface in PECVD system, after a H_2 plasma

treatment for 5 min to reduce the surface oxide of In stripes and allow them to merge into discrete In droplets, at 250 °C with chamber pressure and gas flow rate of 140 Pa and 15 SCCM, respectively. For the a-Si deposition, the precursor gas was SiH_4, with a flow rate of 5 SCCM and a chamber pressure of 20 Pa; (4) finally, the sample was annealed at 350 °C for 60 min in vacuum to activate the In droplets to absorb a-Si and produce crystalline SiNW along their moving course following the predefined guiding edges.

4.2. Bosch-etching of standing Si pillar frames

The positions of the pillars, with a spacing of 50 μm and a diameter of 4 μm, were defined by photolithography. Then, Bosch deep etching procedure was applied in ICP system, with alternating SF_6 etching (100 SCCM, 20 mTorr, 200 W for 13 s) and C_4F_8 passivation (100 SCCM, 20 mTorr, 200 W, 15 s) periods for 120 cycles, to produce standing pillar frame with a depth of about 20 μm, approximately each etching cycle for 200 nm [46].

4.3. 3D Assembly of SiNW slingshot

The transfer and assembly of SiNWs were assisted by using optical fibers installed on the probe stage of a manually-controlled displacement platform, with a length of 15 cm and a tip diameter of ~200 nm. We use the Alcohol burner to ablate the optical fiber and stretch its two ends to make the tip of the optical fiber thinner. The SiNWs were picked up by approaching a fiber tip with tilting angle of 15°, with respect to the ground surface, to the targeted SiNW segment, displacing it from the guiding edge and attaching it more with a suitable contact angle and alignment. Then, the SiNW can be dragged up from the substrate surface and transferred to hook one of the standing pillars, followed by stretching it a little bit to hook connect to the opposite pillar, which can help to impose a little bit tensile stain that will stabilize the NW spring holding firmly on the pillars with fine sidewall grooves.

4.4. Microsphere loading and launching

Microscale SiO_2 spheres of 3–5 μm wide were taken as model payload for the slingshot operation. The microspheres are lifted up by the slim fiber tip, and carried to the proximity of SiNW slingshot. After aligning the fiber tip to the shooting direction and placing the microsphere onto the center cockpit, the optical fiber is controlled to pull back. Due to the adhesive force and frictional dragging between the optical fiber and the SiNW spring, the SiNW spring can be pulled to desired distance for accumulating sufficient mechanical energy. The detaching of spring from fiber tip to trigger slingshot shooting was accomplished by increasing the fiber contact angle or applying a sudden drag. Though these loading and shooting operations are now all controlled manually by experienced operators, it is also possible to pass this manipulation to automated robotic arms, which will bring in more reliability and repeatability. temperature.

Acknowledgments

The authors acknowledge the financial supports received from National Key R&D Program of China (92164201), the National Natural Science Foundation of China under Nos. 61974064, 11874198, 61934004, 62104100, 61921005 and 61934004, and the Fundamental Research Funds for the Central Universities.

Data availability statement

All data that support the findings of this study are included within the article (and any supplementary files).

Author contributions

Conceptualization: Ying Zhang and Linwei Yu; Experiments: Ying Zhang, Dianlun Li, Yongjia Qi and Lei Wu; Analysis: Ying Zhang and Jiang Yan; Simulation: Ying Zhang and Wentao Qian; Visualization: Dianlun Li; Supervision: Zongguang Liu, Junzhuan Wang and Jun Xu; Writing—original draft: Ying Zhang and Linwei Yu; Review and editing: all authors.

ORCID iDs

Jiang Yan https://orcid.org/0000-0002-6079-5058
Junzhuan Wang https://orcid.org/0000-0003-1851-220X
Jun Xu https://orcid.org/0000-0002-0469-9766
Linwei Yu https://orcid.org/0000-0002-0801-5210

References

[1] Gu Y, Chen C, Rufo J, Shen C, Wang Z, Huang P-H, Fu H, Zhang P, Cummer S A and Tian Z 2020 Acoustofluidic holography for micro-to nanoscale particle manipulation *ACS Nano* **14** 14635–45
[2] Johansen P L, Fenaroli F, Evensen L, Griffiths G and Koster G 2016 Optical micromanipulation of nanoparticles and cells inside living zebrafish *Nat. Commun.* **7** 10974
[3] Kim K, Guo J, Liang Z and Fan D 2018 Artificial micro/nanomachines for bioapplications: biochemical delivery and diagnostic sensing *Adv. Funct. Mater.* **28** 1705867
[4] Lee H J, Choi N, Yoon E-S and Cho I-J 2018 MEMS devices for drug delivery *Adv. Drug Deliv. Rev.* **128** 132–47
[5] Lee S, Kim J y, Kim J, Hoshiar A K, Park J, Lee S, Kim J, Pané S, Nelson B J and Choi H 2020 A needle-type microrobot for targeted drug delivery by affixing to a microtissue *Adv. Healthcare Mater.* **9** 1901697
[6] Wang G and Xu Q 2017 Design and precision position/force control of a piezo-driven microinjection system *IEEE/ASME Trans. Mechatron.* **22** 1744–54
[7] Fan Z, Rong W, Tian Y, Wei X and Gao J 2019 Micro-scale droplet deposition for micro-object self-alignment release based on water condensation *Appl. Phys. Lett.* **114** 013703

[8] Shen Y and Fukuda T 2014 State of the art: micro-nanorobotic manipulation in single cell analysis *Robot. Biomimetics* **1** 1–13

[9] Chang B, Sariola V, Jääskeläinen M and Zhou Q 2010 Self-alignment in the stacking of microchips with mist-induced water droplets *J. Micromech. Microeng.* **21** 015016

[10] Feng Y, An M, Liu Y, Sarwar M T and Yang H 2023 Advances in chemically powered micro/nanorobots for biological applications: a review *Adv. Funct. Mater.* **33** 2209883

[11] Fliervoet L A and Mastrobattista E 2016 Drug delivery with living cells *Adv. Drug Deliv. Rev.* **106** 63–72

[12] Wen P, Wu W, Wang F, Zheng H, Liao Z, Shi J, Zhu C, Zhao P, Cheng H and Li H 2023 Cell delivery devices for cancer immunotherapy *J. Control. Release* **353** 875–88

[13] Yi C, Li C-W, Ji S and Yang M 2006 Microfluidics technology for manipulation and analysis of biological cells *Anal. Chim. Acta* **560** 1–23

[14] Mu X, Zheng W, Sun J, Zhang W and Jiang X 2013 Microfluidics for manipulating cells *Small* **9** 9–21

[15] Paunovska K, Loughrey D and Dahlman J E 2022 Drug delivery systems for RNA therapeutics *Nat. Rev. Genet.* **23** 265–80

[16] Faraji A H and Wipf P 2009 Nanoparticles in cellular drug delivery *Bioorganic Medicinal Chem.* **17** 2950–62

[17] Mody V V, Cox A, Shah S, Singh A, Bevins W and Parihar H 2014 Magnetic nanoparticle drug delivery systems for targeting tumor *Appl. Nanosci.* **4** 385–92

[18] Ibsen S, Benchimol M, Simberg D, Schutt C, Steiner J and Esener S 2011 A novel nested liposome drug delivery vehicle capable of ultrasound triggered release of its payload *J. Control. Release* **155** 358–66

[19] Ali U E, Yang H, Khayrudinov V, Modi G, Cheng Z, Agarwal R, Lipsanen H and Bhaskaran H 2022 A universal pick-and-place assembly for nanowires *Small* **18** 2201968

[20] Chen B K, Zhang Y and Sun Y 2009 Active release of microobjects using a MEMS microgripper to overcome adhesion forces *J. Microelectromech. Syst.* **18** 652–9

[21] Lofroth M and Avci E 2019 Development of a novel modular compliant gripper for manipulation of micro objects *Micromachines* **10** 313

[22] Sari I and Kraft M 2015 A MEMS linear accelerator for levitated micro-objects *Sensors Actuators,* A **222** 15–23

[23] Lanier O L, Monsalve A G, McFetridge P S and Dobson J 2019 Magnetically triggered release of biologics *Int. Mater. Rev.* **64** 63–90

[24] Crozier K B 2019 Quo vadis, plasmonic optical tweezers? *Light: Sci. Appl.* **8** 35

[25] Englert C, Nischang I, Bader C, Borchers P, Alex J, Proehl M, Hentschel M, Hartlieb M, Traeger A and Pohnert G 2018 Photocontrolled release of chemicals from nano-and microparticle containers *Angew. Chem. Int. Ed.* **57** 2479–82

[26] Gao X, Cao C, Guo J and Conn A 2019 Elastic electroadhesion with rapid release by integrated resonant vibration *Adv. Mater. Technol.* **4** 1800378

[27] Soto F, Martin A, Ibsen S, Vaidyanathan M, Garcia-Gradilla V, Levin Y, Escarpa A, Esener S C and Wang J 2016 Acoustic microcannons: toward advanced microballistics *ACS Nano* **10** 1522–8

[28] Ranallo S, Prévost-Tremblay C, Idili A, Vallée-Bélisle A and Ricci F 2017 Antibody-powered nucleic acid release using a DNA-based nanomachine *Nat. Commun.* **8** 15150

[29] Zhang H, Tersoff J, Xu S, Chen H, Zhang Q, Zhang K, Yang Y, Lee C-S, Tu K-N and Li J 2016 Approaching the ideal elastic strain limit in silicon nanowires *Sci. Adv.* **2** e1501382

[30] Kataria D, Kumar S, Balguvhar S, Mukhiya R, Jain A, Kumar S S and Sinha S 2017 International Conference on Recent Innovations in Signal processing and Embedded Systems (RISE)

[31] O'Mara W, Herring R B and Hunt L P 2007 *Handbook of Semiconductor Silicon Technology* (South Africa: Crest Publishing House)

[32] Zhu Y, Xu F, Qin Q, Fung W Y and Lu W 2009 Mechanical properties of vapor−liquid−solid synthesized silicon nanowires *Nano Lett.* **9** 3934–9

[33] Yu L, Alet P-J, Picardi G and I Cabarrocas P R 2009 An in-plane solid−liquid−solid growth mode for self-avoiding lateral silicon nanowires *Phys. Rev. Lett.* **102** 125501

[34] Yu L, Oudwan M, Moustapha O, Fortuna F and Roca i Cabarrocas P 2009 Guided growth of in-plane silicon nanowires *Appl. Phys. Lett.* **95** 113106

[35] Xue Z, Sun M, Dong T, Tang Z, Zhao Y, Wang J, Wei X, Yu L, Chen Q and Xu J 2017 Deterministic line-shape programming of silicon nanowires for extremely stretchable springs and electronics *Nano Lett.* **17** 7638–46

[36] Westerman R, Martinez L, Pays-Volard D, Mackenzie K and Lazerand T 2014 *Deep Silicon Etching: Current Capabilities And Future Directions* vol 8973 (SPIE) pp 38–51

[37] Kirsch V 2003 Calculation of the van der Waals force between a spherical particle and an infinite cylinder *Adv. Colloid Interface Sci.* **104** 311–24

[38] Rosenfeld J and Wasan D 1974 The London force contribution to the van der Waals force between a sphere and a cylinder *J. Colloid Interface Sci.* **47** 27–31

[39] Ku B, van de Wetering F, Bolten J, Stel B, van de Kerkhof M A and Lemme M C 2023 AFM-based hamaker constant determination with blind tip reconstruction *Adv. Mater. Technol.* **8** 2200411

[40] Šafarič R and Lukman D 2014 One-finger gripper based on the variable van der Waals force used for a single nano/micro-sized object *J. Micromech. Microeng.* **24** 085012

[41] Paulus B C, Banh J K, Rector K D, Stein B W and Lilley L M 2022 Whispering gallery mode resonators in continuous flow: spectral assignments and sensing with monodisperse microspheres *Anal. Methods* **14** 1690–7

[42] Jones C H, Chen C-K, Ravikrishnan A, Rane S and Pfeifer B A 2013 Overcoming nonviral gene delivery barriers: perspective and future *Mol. Pharm.* **10** 4082–98

[43] Liu Z, Yan J, Ma H, Hu T, Wang J, Shi Y, Xu J, Chen K and Yu L 2021 *Ab initio* design, shaping, and assembly of free-standing silicon nanoprobes *Nano Lett.* **21** 2773–9

[44] Wang B, Kostarelos K, Nelson B J and Zhang L 2021 Trends in micro-/nanorobotics: materials development, actuation, localization, and system integration for biomedical applications *Adv. Mater.* **33** 2002047

[45] Yan J, Zhang Y, Liu Z, Wang J, Xu J and Yu L 2023 Ultracompact single-nanowire-morphed grippers driven by vectorial Lorentz forces for dexterous robotic manipulations *Nat. Commun.* **14** 3786

[46] Ma H, Yuan R, Wang J, Shi Y, Xu J, Chen K and Yu L 2020 Cylindrical line-feeding growth of free-standing silicon nanohelices as elastic springs and resonators *Nano Lett.* **20** 5072–80